Quantitative analysis of depolarization of backscattered light by stochastically inhomogeneous dielectric particles

Xu Li, Allen Taflove, and Vadim Backman

Department of Biomedical Engineering and Department of Electrical and Computer Engineering, Northwestern University, Evanston, Illinois 60208

Received October 25, 2004

We determine the relationship between the depolarization properties of inhomogeneous particles and the statistical parameters of their internal refractive-index distributions. Our analysis demonstrates that the linear depolarization ratio of backscattered light by an inhomogeneous particle is approximately proportional to both the squared standard deviation and the squared correlation length of the particle's internal refractive-index distribution. We verify this result by conducting rigorous numerical studies using the finite-difference time-domain method. This improved understanding of light depolarization by inhomogeneous structures may enhance polarization-based biomedical optical imaging techniques. © 2005 Optical Society of America

OCIS codes: 290.1350, 260.5430, 290.5850.

Understanding polarized light propagation in inhomogeneous media is essential for applications in areas such as biomedical optical imaging. Extensive studies have been devoted to investigating the polarization state of light after multiple scattering events, i.e., the scrambling effect.[1] A number of researchers have investigated the depolarization effect of nonspherical and inhomogeneous particles.[2] The importance of this type of investigation is twofold. First, the linear or circular depolarization ratio can potentially be used to characterize the particle's nonsphericity and inhomogeneity since a homogeneous spherical particle does not change the polarization state of backscattered light. Second, understanding the depolarizing effect of single nonspherical and inhomogeneous particles is essential for improvement of the analysis of light scattering by random media.

In this Letter we investigate the depolarization effect of dielectric particles with complex internal structures. The polarized light-scattering properties of such particles have significant relevance to applications in optical tissue diagnosis and imaging on the subcellular level, such as polarized light-scattering spectroscopy[3] and polarized reflectance microscopy.[4] We systematically investigate the depolarization effect of a wide variety of inhomogeneous particles with complex internal structures. Both our numerical experiments and theoretical analysis demonstrate that the backscattered linear depolarization ratio is directly associated with the statistical parameters of the particle's internal geometry, including the standard deviation of the refractive index and the correlation length of the inhomogeneity.

Our numerical study is based on the finite-difference time-domain (FDTD) method,[5] which solves the Maxwell's equations numerically and therefore provides accurate benchmark data for light-scattering problems involving complex particle geometries.[6] We adopt a stochastic model, the Gaussian random field (GRF) model,[7] to describe the geometry of the complex internal structure of inhomogeneous particles. The spatial distribution statistics of a GRF variable [refractive index $n(\mathbf{r})$ in our case] is uniquely determined by two statistical parameters: standard deviation of the refractive index σ_n and correlation length L_c. Following the procedures described in Ref. 7, we numerically generate inhomogeneous dielectric spheres with a range of values of σ_n and L_c, fixed volume-averaged refractive index $n_0 = 1.1$, and diameter $D = 4.0$ μm. Figure 1 graphs six representative particles with refractive-index distributions synthesized by the GRF model. In each example, we map the $\hat{\mathbf{x}}-\hat{\mathbf{z}}$ cross-sectional cut of the particle's interior refractive-index distribution in gray scale. In Figs. 1(a)–1(c), σ_n is fixed around 0.02 and L_c increases from 0.1 [Fig. 1(a)] to 1.2 μm [Fig. 1(c)]. In Figs. 1(d) and 1(e), L_c is fixed at 400 nm and σ_n increases from 0.01 [Fig. 1(d)] to 0.03 [Fig. 1(f)]. These examples demonstrate the capability of the GRF model to mimic refractive-index fluctuations occurring over a variety of geometric scales. It is evi-

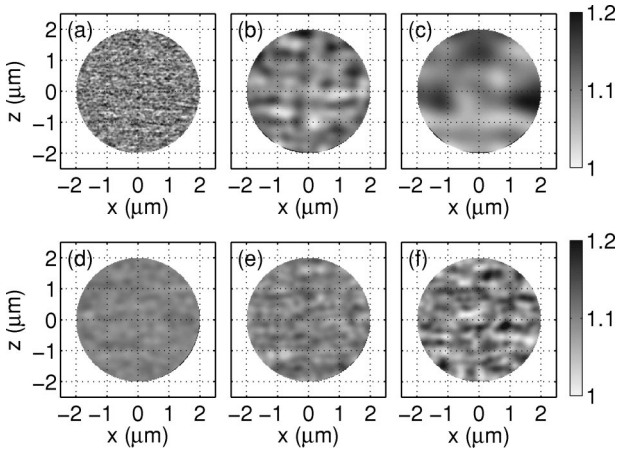

Fig. 1. Examples of inhomogeneous spherical particles with GRF refractive-index distributions with fixed $n_0 = 1.1$ and $D = 4$ μm but a variety of values of L_c and σ_n: (a) $L_c = 0.1$ μm, $\sigma_n = 0.02$; (b) $L_c = 0.6$ μm, $\sigma_n = 0.02$; (c) $L_c = 1.2$ μm, $\sigma_n = 0.02$; (d) $L_c = 0.4$ μm, $\sigma_n = 0.012$; (e) $L_c = 0.4$ μm, $\sigma_n = 0.024$; (f) $L_c = 0.4$ μm, $\sigma_n = 0.032$.

0146-9592/05/080902-3/$15.00

dent that σ_n describes the magnitude of refractive-index variability, whereas L_c characterizes the size of the internal features of the particle.

The geometries of the GRF-synthesized inhomogeneous particles are imported to the FDTD grid with a staircasing scheme with 25-nm resolution. We use the pure scattered-field scheme[5] to excite an impulse $\hat{\mathbf{x}}$-polarized plane wave propagating in the $\hat{\mathbf{z}}$ direction within the FDTD grid. The scattered-field frequency response for a 500–1000-nm incident wavelength range is extracted by means of a discrete Fourier transform from the time-domain data recorded on the near-field surfaces and normalized by the spectrum of the source pulse. A modified three-dimensional near-to-far field transformation[8] in the phasor domain is implemented to calculate the far-field scattered wave in the backward direction for both copolarized ($E_{\parallel}$) and cross-polarized ($E_{\perp}$) responses.

Figure 2 shows three representative results of our numerical experiments. In each example the spatial distribution of the particle refractive index in one cross-sectional cut is displayed on the left, and the backscattered intensities in both polarizations ($I_{\parallel}$ and $I_{\perp}$) calculated with the FDTD method are graphed on the right. Ignoring the oscillatory structures caused by resonance in the backscattered spectra, it is clear that the overall level of $I_{\perp}$, and therefore linear depolarization ratio $\delta_l \equiv I_{\perp}/I_{\parallel}$, increases as L_c and σ_n become larger.

The following analysis provides an interpretation of the dependence of the depolarization effect on the geometric parameters of inhomogeneous particles. Here we assume an inhomogeneous spherical particle centered at $\mathbf{r}=0$ being illuminated by incident light linearly polarized along the $\hat{\mathbf{x}}$ axis and propagating along the $\hat{\mathbf{z}}$ direction. Similar to the Wentzel–

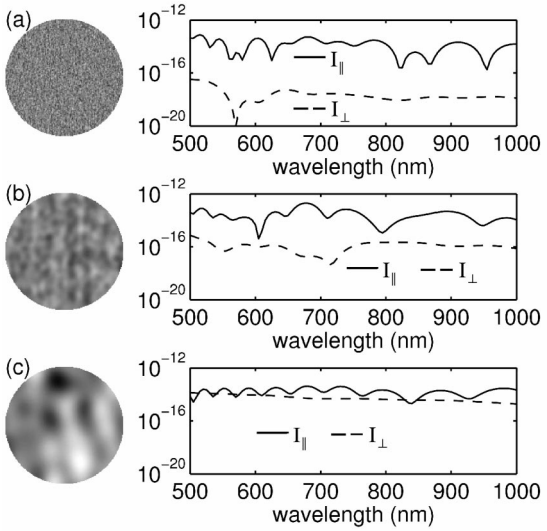

Fig. 2. Demonstration that the overall intensity of cross-polarized backscattering light increases as $L_c\sigma_n$ becomes greater. Here copolarized and cross-polarized backscattering light intensity are calculated by the FDTD method for inhomogeneous dielectric spheres with $n_0=1.1$, $D=4$ μm, and a variety of L_c and σ_n: (a) $L_c=0.05$ μm, $\sigma_n=0.02$; (b) $L_c=0.4$ μm, $\sigma_n=0.016$; (c) $L_c=1.2$ μm, $\sigma_n=0.035$.

Kramers–Brillouin analysis,[6,7] we start our analysis by examining the optical path and the associated phase change of a specific light ray entering the particle at position (r,φ) and exiting at $(r,\varphi+180°)$ projected to the $\hat{\mathbf{x}}$–$\hat{\mathbf{y}}$ plane. Then the $\hat{\mathbf{r}}$–$\hat{\mathbf{z}}$ plane becomes the plane of propagation of the light ray. We split both the incident field $\mathbf{E}_i$ and the far-field backscattered field $\mathbf{E}_s$ into the parallel component E_a and perpendicular component E_e with respect to the $\hat{\mathbf{r}}$-$\hat{\mathbf{z}}$ plane. If scattering outside this plane is neglected, the backscattered field can be represented by $E_{a,s}(r,\varphi)=s_2(r,\varphi)E_{a,i}$ and $E_{e,s}(r,\varphi)=s_1(r,\varphi)E_{e,i}$. Note that for each light ray the incident field may have both parallel and perpendicular components with respect to the propagation plane. The total backscattered field is the summation of the contributions from all the light rays with $0\leqslant\varphi\leqslant 2\pi$. The combination of scattered fields associated with two orthogonal scattering planes with $\varphi=\varphi_0$ and $\varphi=\varphi_0+\pi/2$ is given by $\mathbf{E}_{\mathrm{st}}(r,\varphi_0)=\mathbf{E}_s(r,\varphi_0)+\mathbf{E}_s(r,\varphi_0+\pi/2)$. Since $E_{a,e}(r,\varphi)=E_{e,a}(r,\varphi+\pi/2)$, we have $E_{a,\mathrm{st}}(r,\varphi)=\{s_2(r,\varphi)+s_1[r,\varphi+(\pi/2)]\}E_{a,i}$ and $E_{e,\mathrm{st}}(\mathrm{r},\varphi)=\{s_1(r,\varphi)+s_2[r,\varphi+(\pi/2)]\}E_{e,i}$. Thus the cross-polarized ($\hat{\mathbf{y}}$) component of scattered field $E_{\perp,\mathrm{st}}(r,\varphi)$ is given by

$$E_{\perp,\mathrm{st}}(r,\varphi)=E_i\{s_2(r,\varphi)-s_2[r,\varphi+(\pi/2)]+s_1(r,\varphi)-s_1[r,\varphi+(\pi/2)]\}\cos\varphi\sin\varphi. \quad (1)$$

Total cross-polarized intensity $I_{\perp}$ can be expressed as $\propto|\int_0^{D/2}\int_0^{\pi}E_{\perp,\mathrm{st}}(r,\varphi)r\mathrm{d}r\mathrm{d}\varphi|^2$.

If a particle is azimuthally symmetrical, then $S_{1,2}(r,\varphi)=S_{1,2}[r,\varphi+(\pi/2)]$, and thus $E_{\perp,\mathrm{st}}=0$. This does not hold generally, however, for internally inhomogeneous particles. Because of the variation of the refractive index within the particle, photons propagating in scattering planes defined by azimuth angles φ and $\varphi+(\pi/2)$ travel different optical paths and therefore have a phase difference of Δf. To account for this effect, we write $s_{1,2}[r,\varphi+(\pi/2)]\approx s_{1,2}(r,\varphi)\exp(i\Delta f)$. Therefore the linear depolarization ratio, defined as $\delta_l\equiv I_{\perp}/I_{\parallel}$, can be estimated as

$$\delta_\ell\approx\frac{1}{4\pi^2 I_{\parallel}}\left|\int_0^{D/2}[s_2(r)-s_1(r)]r\mathrm{d}r\times\int_0^{\pi}\mathrm{d}\varphi\cos\varphi\sin\varphi[1-\exp(i\Delta f)]\right|^2. \quad (2)$$

Note that phase difference Δf is proportional to the optical path-length difference of the light rays; i.e., $\Delta f=(2\pi/\lambda)\int\Delta n\mathrm{d}l$, where Δn is defined as $\Delta n\equiv n(\varphi)-n[\varphi+(\pi/2)]$, and the integration is performed over the path of the photon. Since internal refractive index n can be considered constant within correlation length L_c, the integration can be replaced by a summation as $\Delta f\approx(2\pi/\lambda)\Sigma_i^N\Delta n_i L_c$, where $N=2D/L_c$. If the standard deviation of Δf satisfies

$$\sigma_{\Delta f}\approx(4\sqrt{2}\pi/\lambda)(DL_c)^{1/2}\sigma_n<1, \quad (3)$$

the exponential in expression (2) can be expanded in Δf, and the expectation of the second integral in

expression (2) can be estimated as

$$\left\langle \left| \int \mathrm{d}\varphi \cos\varphi \sin\varphi [1 - \exp(i\Delta f)] \right|^2 \right\rangle \approx \left\langle \left| (4\pi/\lambda) \sum_{i,j}^{NM} \cos\varphi_j \sin\varphi_j \Delta n_{ij} L_c^2 / D \right|^2 \right\rangle,$$

with $M = \pi D / L_c$. To further simplify expression (2), we estimate

$$\langle |\sum_{i,j}^{NM} \cos\varphi_j \sin\varphi_j \Delta n_{ij}|^2 \rangle \approx \langle |\sum_{i,j}^{NM} \cos^2\varphi_j \sin^2\varphi_j (\Delta n_{ij})^2| \rangle \propto (\pi/2)(\sigma_n D/L_c)^2.$$

Substituting the above expressions into expression (2), we obtain

$$\delta_l \approx C(2\pi/\lambda^2)(L_c\sigma_n)^2, \tag{4}$$

where C is a constant independent of the distribution of the internal refractive index. Note that this expression for δ_l results from expanding the exponential in expression (2) to its first-order term. Following a similar approach, we can obtain the second-order term in the expansion of δ_l as $\delta_l^{(2)} \propto -6\pi^3 (L_c\sigma_n/\lambda)^4$. This term is always negative and tends to be small if $L_c\sigma_n/\lambda < 1$. Therefore, for a wide range of inhomogeneous particles, δ_l is proportional to both σ_n^2 and L_c^2 according to expression (4).

Expression (4) provides an explicit expression for associating backscattered linear depolarization ratio δ_l of an inhomogeneous particle with the statistics of its internal structure. This relation agrees with the observation from the numerical results presented in Fig. 2. It is further substantiated by our comprehensive numerical experiments conducted on a wide variety of inhomogeneous dielectric spheres. Figure 3 summarizes our FDTD numerical results for 20 inhomogeneous dielectric spheres with L_c ranging from 0.05 to 1.2 μm and $\sigma_n/(n_0 - 1)$ ranging from 0.05 to 0.36. Here we plot δ_l averaged over the 500–1000-nm incident wavelength range against the geometric parameter $\bar{\beta} \equiv C(2\pi/\bar{\lambda}^2)(L_c\sigma_n)^2$ in a logarithmic scale to cover a wide range for both parameters. Constant C in expression (4) is chosen empirically as $C = 12$ to give the best linearity. The 20 data points are plotted with symbols representing different L_c and gray-scale levels corresponding to different σ_n for each particle geometry. We also cross reference three data points with their corresponding backscattered spectra shown in Figs. 2(a)–2(c). The relationship given in expression (4) is plotted as a dashed line to compare against the data points. The reasonable data fitting confirms the validity of expression (4); i.e., $\delta_l \propto (2\pi/\lambda^2)(L_c\sigma_n)^2$ for the first order of approximation.

In summary, our analytical and numerical investigation has demonstrated that the linear depolarization ratio of light backscattered from inhomogeneous particles is approximately proportional to both the squared standard deviation and squared correlation length of internal refractive-index distribution. This relation provides us with a straightforward means to quantify the depolarization effect of inhomogeneous particles. It may also assist the analysis and characterization of particle microstructures using polarized light scattering or imaging techniques.

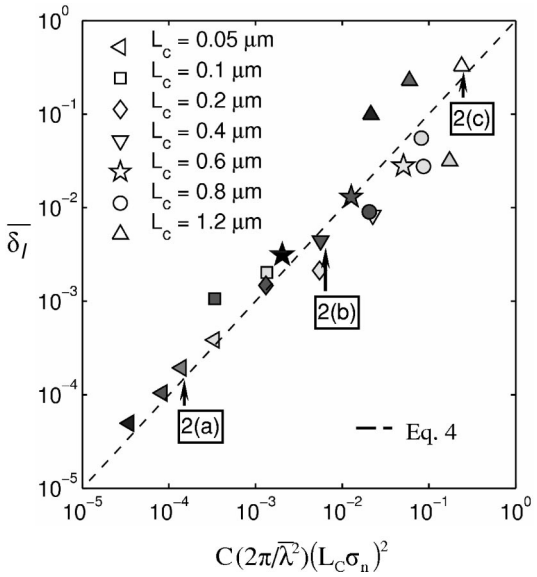

Fig. 3. Confirmation of the validity of expression (4), i.e., that δ_l is approximately proportional to $(2\pi/\lambda)(L_c\sigma_n)^2$. Here the averaged linear depolarization ratio is calculated from FDTD simulations conducted on 20 inhomogeneous dielectric spheres as a function of geometric parameter $\beta \equiv C(2\pi/\bar{\lambda}^2)(L_c\sigma_n)^2$, with L_c ranging from 0.05 to 1.2 μm and σ_n ranging from 0.005 to 0.035. In the calculation of β we chose $C = 12$ and $\bar{\lambda} = 750$ nm. The gray-scale level of each data point represents the magnitude of σ_n with the brighter shades corresponding to greater σ_n.

This study was supported by National Science Foundation grants BES-0238903 and ACI-0219925. The computational resources were provided by the National Science Foundation Teragrid under grant MCB040062N. X. Li's e-mail address is xuli@northwestern.edu.

References

1. C. Brosseau, *Fundamentals of Polarized Light: a Statistical Optics Approach* (Wiley, New York, 1998).
2. M. I. Mishchenko and J. W. Hovenier, Opt. Lett. **20**, 1356 (1995).
3. H. K. Roy, Y. Liu, R. K. Wali, Y. L. Kim, A. K. Kromine, M. J. Goldberg, and V. Backman, Gastroenterology **126**, 1071 (2004).
4. M. Rajadhyaksha, S. Gonzalez, and J. M. Zavislan, J. Biomed. Opt. **9**, 323 (2004).
5. A. Taflove and S. Hagness, *Computational Electrodynamics: the Finite-Difference Time-Domain Method* (Artech House, Norwood, Mass., 2000).
6. X. Li, Z. Chen, A. Taflove, and V. Backman, Appl. Opt. **43**, 4497 (2004).
7. X. Li, Z. Chen, A. Taflove, and V. Backman, Phys. Rev. E **70**, 056610 (2004).
8. X. Li, A. Taflove, and V. Backman, "Modified FDTD near-to-far field transformation for improved backscattering calculation of strongly forward-scattering objects," IEEE Antennas Wireless Propag. Lett. (to be published).